LA-UR-98-6566-Rev. 1
August 28, 2000

Title: **PROCESS DESIGN FOR THERMAL INDUCED GALLIUM REMOVAL (TIGR) FROM PLUTONIUM OXIDE**

Author: Scott F. DeMuth

Submitted to: General Distribution

Los Alamos
NATIONAL LABORATORY

PROCESS DESIGN FOR THERMAL INDUCED GALLIUM REMOVAL (TIGR) FROM PLUTONIUM OXIDE

August 28, 2000

Scott F. DeMuth

Los Alamos National Laboratory

Los Alamos, NM U.S.A.

Keywords

MOX, TIGR

Gallium, Plutonium

ABSTRACT

The use of mixed oxide (MOX) fuel for disposition of plutonium derived from weapons is one option for nuclear disarmament in the United States and Russia. Fabrication of MOX fuel with plutonium derived from weapons must conform to current accepted nuclear fuel specifications if the related fuel licensing effort is to be minimized. It has been determined that MOX fuel prepared with plutonium derived from weapons could have a gallium concentration in excess of MOX fuel currently licensed in Europe. Thermal Induced Gallium Removal (TIGR) has been proposed as a dry method to separate gallium from plutonium oxide by vaporization. This study was initiated in order to determine the advantages of using a mixed-bed rather than a fixed-bed furnace for separation of gallium from PuO_2 by the TIGR process. Since a fixed-bed furnace is less complex; and consequently, less expensive to fabricate and operate, strong evidence for the use of a mixed-bed furnace is necessary to purse its development. The results of this study indicate that a mixed-bed furnace would provide no significant advantage over a fixed-bed.

NOMENCLATURE

a	activity
A	interfacial mass transfer area
$\overline{C}$	molar concentration averaged over the particle radius
$C_{i,R}$	molar concentration of "i" at surface of particle in the solid phase
$C_{i,max}$	maximum possible concentration of "i" in solid phase, in equilibrium with gas phase
d_p	particle diameter
D	diffusion coefficient
ΔH^o	change in enthalpy
ΔG	change in Gibbs free energy
$k_{ad,i}$	adsorption equilibrium constant
$k_{g,i}$	gas-phase mass transfer coefficient for component "i"
K_f	forward chemical reaction rate constant
K_b	backward chemical reaction rate constant
K_{eq}	equilibrium constant for reaction
m_i	mass of species "i"
M	mole weight
$M_{g,\infty}$	bulk gas mole weight
N_i	moles of component "i"
N_{sh}	Sherwood number
N_{sc}	Schmidt number
N_{re}	Reynolds number
P	pressure
$P_{i,R}$	pressure of component "i" at surface of sphere with radius "R"
$P_{i,\infty}$	pressure of component "i" in bulk gas stream
P_t	total gas pressure in bulk gas stream
r	radius
R	universal gas constant
t	time
T	temperature
$v_{g,\infty}$	bulk gas velocity
V	volume
X	mole fraction
Δy	distance over which diffusion occurs (i.e. boundary layer thickness)
ε	extent of reaction
γ	activity coefficient
ρ	mass density
$\rho_{g,\infty}$	bulk gas mass density
$\mu_{g,\infty}$	bulk gas viscosity
σ	hard-sphere diameter
∇	laplacian
erf	error function

INTRODUCTION

The ratified START I, nearly ratified START II, and proposed START III Treaties are currently the backbone of the joint United States (U.S.) and Russian plan for nuclear disarmament. The START agreements will reduce the number of strategic nuclear delivery vehicles and associated warheads. START I reduces the deployed nuclear arsenals of the U.S. and Russia to approximately 6000 each, and START II is intended to further reduce the deployed nuclear arsenals to 3000-3500 each. START III was originally intended to reduce arsenals to 2000-2500 each; however, Russia has recently indicated a desire to reduce further to approximately 1500 each.

The START I Treaty was ratified by both the U.S. and Soviet Union in July 1991 and entered into force December 1994. The START II Treaty was ratified by the U.S. Senate January 1996 and only recently by the Russian Duma. To facilitate Duma approval a summit was held in March 1997 at Helsinki which resulted in a number of Amendments to START II. In ratifying START II the Duma reaffirmed a number of important requirements. Russia's continued adherence to START II is dependent on the U.S. adherence to the Anti Ballistic Missile (ABM) Treaty and to completion of a START III. The Russians have stated in their resolution of ratification that they will not exchange the instruments of ratification bringing START II into agreement until the U.S. Senate approves the Helsinki Amendments. (Journal of Arms Control Today, May 2000)

Not addressed by the START Treaties is the disposition of nuclear materials following warhead dismantlement. While the START Treaties reduce the immediate threat of nuclear weapons, the nuclear materials can be reused in future weapons if not destroyed. A program is being developed jointly by the U.S. and Russia to permanently disposition excess weapons related nuclear materials. In particular, it has been agreed upon by the U.S. and Russia that approximately 35-50 MT of weapons related plutonium be dispositioned by each side. Two methods of plutonium dispositioning have been tentatively agreed upon, (1) incorporation of plutonium into mixed oxide (MOX) nuclear reactor fuel for power generation, and (2) immobilization of plutonium with highly radioactive waste followed by disposal in a deep underground repository. The U.S. currently plans on using approximately 2/3 of the 35-50 MT for MOX fuel, with the remainder to be disposed in a repository such as Yucca Mountain (The White House, Office of the Press Secretary, 1 September 1998). Plutonium to be dispositioned by MOX fuel is more pure than that to be dispositioned in the repository.

One of the most difficult materials to properly disposition is plutonium. The final dispositioned form must provide adequate immobilization for centuries as well as make theft very difficult. One method of plutonium disposition is to combine plutonium oxide with depleted or natural uranium oxide as a nuclear fuel. Following power generation, the spent MOX fuel serves as an immobilized form, the highly radioactive fission products make theft of the remaining plutonium very difficult, and the change in plutonium isotopic distribution makes its future use as weapons material less attractive. Another method is to

encase plutonium in highly radioactive material, such as waste derived from the original production of plutonium, and then store in an underground repository. The highly radioactive material makes theft and future use very difficult and expensive.

As previously stated, the United States Department of Energy (DOE) Fissile Material Disposition Program is based in part on the disposition of plutonium by mixed oxide (MOX) fuel irradiation in commercial light water reactors (LWRs) (see Figure 1). Plutonium derived from weapons is converted to PuO_2 and combined with UO_2 to form the MOX fuel. While commercial LWRs in the United States currently are not licensed for the use of MOX fuel, many are in Europe. Consequently, the European experience will be used as the basis for licensing the fuel in United States. The European experience indicates that MOX fuel fabricated directly with plutonium derived from weapons could require a significant new fuel qualification program for licensing due to the gallium concentration. Because a significant new fuel qualification program would be costly and time consuming, it has been decided that the gallium should be removed from the plutonium prior to fuel fabrication. Thermal Induced Gallium Removal has been proposed as a dry process for removing the gallium.

Since TIGR process development has recently been discontinued and is now considered a backup gallium separation method, this report has been prepared as an archive of its state of process modeling at the time of development termination. The purpose behind the process modeling was to determine if a clear advantage could be achieved with the use of mixed-bed

rather than fixed-bed processing. The use of a mixed-bed will introduce greater design and operational complexities than the use of a fixed-bed. These complexities are further increased by the need to carefully contain the PuO_2.

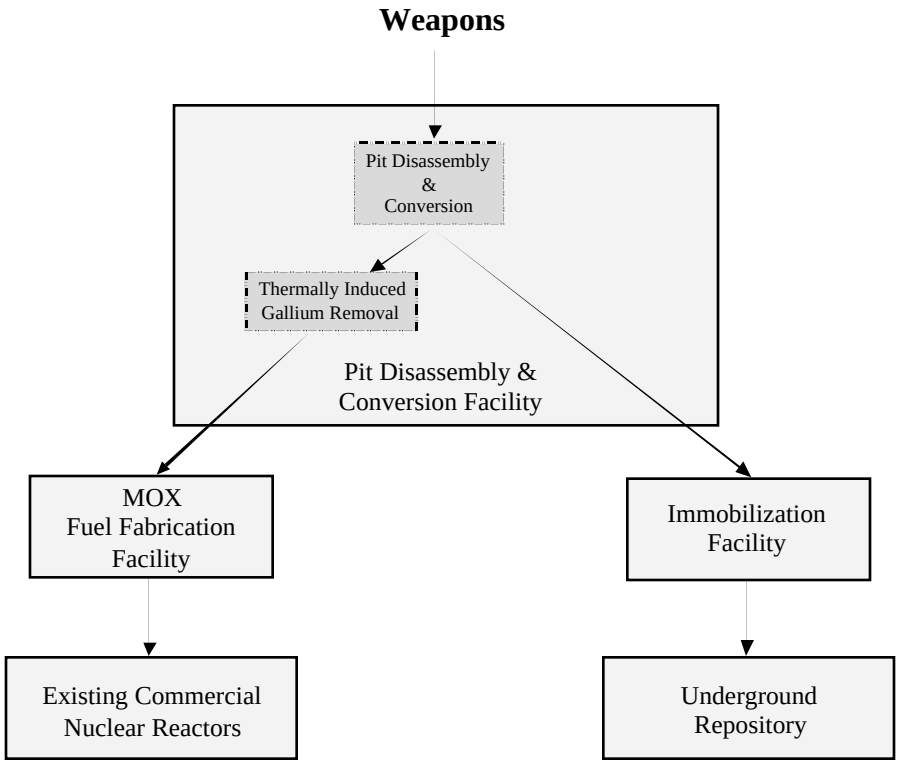

Figure 1. United States plutonium disposition program

SUMMARY

The purpose of this study was to determine without extensive PuO_2 testing whether or not a significant advantage exists for the use of a mixed-bed rather than fixed-bed furnace for gallium separation from PuO_2 by the TIGR process. It can be concluded from this study that there is no significant advantage for using a mixed-bed rather than a fixed-bed furnace. This is based upon the conclusion that at early times the gallium separation rate is dictated by mass transfer in the gas phase, and at long times it is dictated by diffusion within the particle. In order to obtain a reasonable processing time the temperature must be high enough to limit the affect of diffusion within the particle, which tends to reduce the impact of mass transfer in the gas phase at early times. The use of a mixed-bed rather than a fixed-bed does not provide any significant advantage since the affect of mass transfer in the gas phase minimal,

An additional important conclusion derived from this study is that either (1) particle pre-grinding, (2) a temperature in excess of 1500 K or (3) a combination of pre-grinding and temperature increase will be likely be required to achieve a reasonable processing time. This is important because (1) pre-grinding increases PuO_2 containment difficulties and (2) ~1500 K is the maximum operating temperature at which the use of conventional materials for the furnace fabrication is possible.

ANALYSES

The analysis was divided into the following three categories in order to provide a process model that was complete, yet simple enough for reasonable mathematical solutions.

(1) Conceptualization of all potential processing mechanisms
(2) Pre-selection of the most significant processing mechanisms
(3) Solution of the simplified models and comparison of the most significant processing mechanisms

(1) **Conceptualization of all Potential Processing Mechanisms**

Upon conversion of weapons based metallic plutonium (with ≤ 1 wt% Ga) to PuO_2, the gallium is converted to predominantly Ga_2O_3 (see Figure 11 of Kolman, 1999). The gallium is then removed through chemical reduction of the $(Ga_2O_3)_{solid}$ with hydrogen to form the volatile suboxide $(Ga_2O)_{gas}$. Proposed mechanisms involved in the TIGR process are shown in Figure 2. The sequence and description of these mechanisms are as follows.

(i) Adsorption of hydrogen from the gas phase to the solid PuO_2 phase as described by Langmuir's isotherm
(ii) Diffusion of hydrogen into the solid PuO_2 phase
(iii) Chemical reduction of Ga_2O_3 to Ga_2O
(iv) Diffusion of Ga_2O out of the solid PuO_2 phase

(v) Convective mass transfer of Ga_2O from the particle surface to the bulk gas

(2) Pre-selection of the most Significant Processing Mechanisms

The concentration of hydrogen in the gas phase is 6 vol% in argon and constantly replenished at a velocity of approximately 6 cm/s. Since the diffusion of hydrogen in the gas or solid phase should be significantly greater than that of gallium trioxide or the its suboxide, the gallium separation rate should not be dictated by the hydrogen adsorption or hydrogen diffusion within the particle.

Additionally, the principal investigators reported that the hydrogen partial pressure does not significantly affect the gallium separation rate from PuO_2 (Kolman, 1998). It is shown in Figure 2 that the hydrogen partial pressure dictates the hydrogen concentration in the PuO_2 by way of adsorption as described by Langmuir's isotherm. Furthermore, the square of the hydrogen concentration in the particle does affect the chemical kinetics as shown by the reaction rate expression. Consequently, the chemical kinetics do not affect the gallium separation rate as determined by its lack of dependency on the hydrogen partial pressure.

Two possible mechanisms remain that can control the gallium separation rate. The first mechanism is that of gallium diffusion within the solid particle, and the second mechanism is that of gallium suboxide (Ga_2O) mass transfer in

the gas phase. Furthermore, it will be shown later that it is the diffusion of Ga_2O rather than Ga_2O_3 that is of primary significance within the particle.

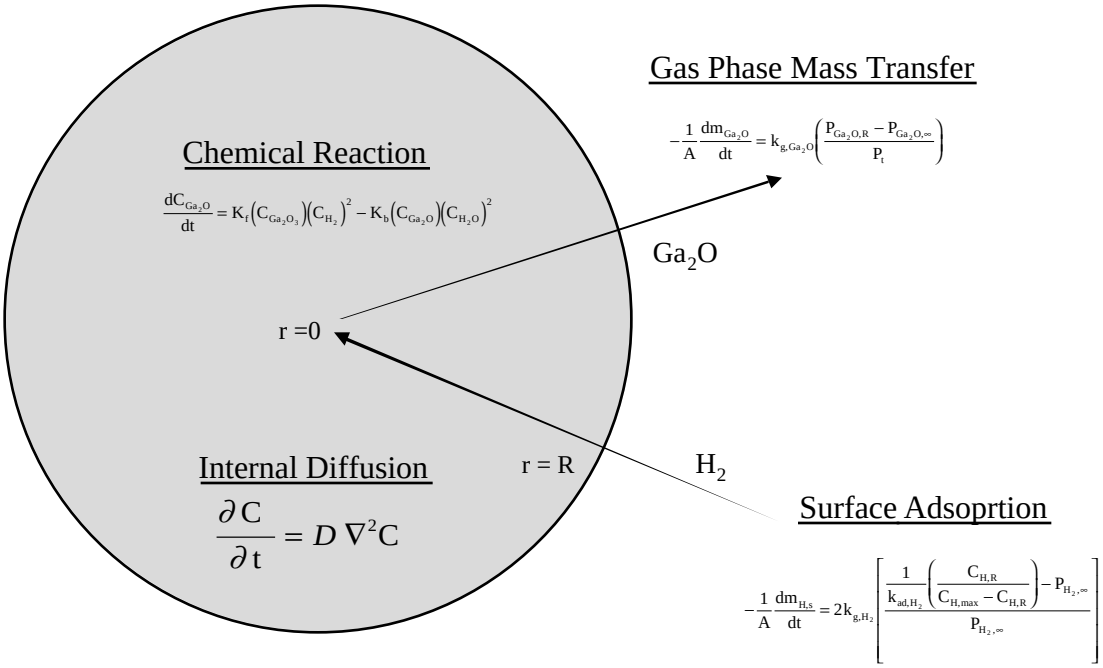

Figure 2. Potential mechanisms of the TIGR process

(3) Detailed Modeling and Comparison of the most Significant Processing Mechanisms

(3.1) Gallium Suboxide (Ga_2O) Convective Mass Transfer from the Particle Surface to the Bulk Gas

The gallium suboxide mass transfer rate in the gas phase has been modeled by film theory for this study. Equation 1 defines the basis for gas phase mass transfer where the film thickness Δy can be further defined by boundary layer theory for convective mass transfer.

$$-\frac{1}{A}\left(\frac{dN_{Ga_2O}}{dt}\right) = D_{Ga_2O}\frac{dC}{dy}$$

or

$$-\frac{1}{A}\left(\frac{dN_{Ga_2O}}{dt}\right) = k_{g,Ga_2O}\frac{\Delta P_{Ga_2O}}{P_t}$$

where

$$P_{Ga_2O,\infty} \approx 0$$

and

$$k_{g,Ga_2O} \propto \frac{D_{Ga_2O}}{\Delta y} \qquad \text{Eq. 1}$$

The gallium suboxide partial pressure is represented here by Equation 2, as modified from Equation 4 of Trellue.

$$Ga_2O_3(s) + 2H_2(s) \rightarrow Ga_2O(g) + 2H_2O(g)$$

$$\frac{\left(a_{Ga_2O,g}\right)\left(a_{H_2O,g}\right)^2}{\left(a_{Ga_2O_3,s}\right)\left(a_{H_2,g}\right)^2} = e^{\frac{-RT}{\Delta G}}$$

$$\frac{P_{Ga_2O}P_{H_2O}^2}{\left(\gamma_{Ga_2O_3}X_{Ga_2O_3}\right)P_{H_2}^2} = e^{\frac{-RT}{\Delta G}} \qquad \text{Eq. 2}$$

where

$$\frac{-RT}{\Delta G} = 91.4 + (0.00112)T - \left(7.76x10^{-8}\right)T^2 - \frac{64,200}{T} + \frac{158,000}{T^2} - (7.81)\ln(T)$$

If it is assumed the gallium separation rate is solely dictated by mass transfer in the gas phase, then the gallium concentration in the PuO_2 solid phase is homogeneous as shown by Figure 3. For conditions of gas phase mass transfer control, Equation 3 represents the gallium concentration in the solid PuO_2 phase as a function of time.

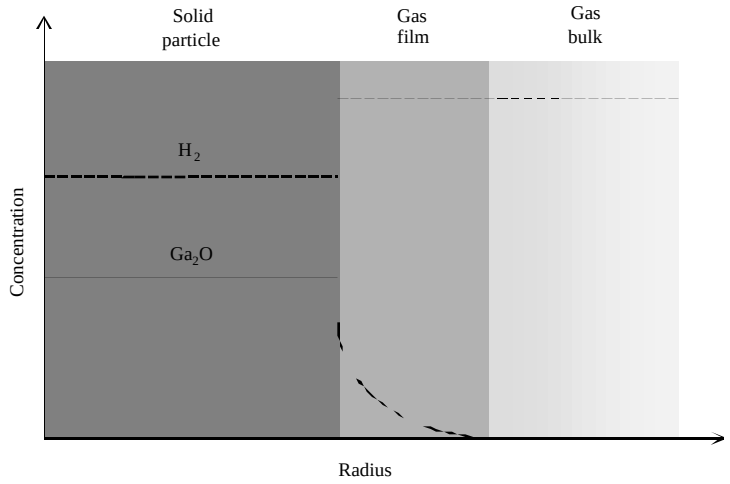

Figure 3. Concentration profiles for gas phase mass transfer control

$$\frac{d\left(N_{Ga_2O_3,particle}\right)}{dt} = \frac{d\left(N_{Ga_2O,gas}\right)}{dt} = \frac{1}{2}\frac{d\left(N_{H_2O,gas}\right)}{dt}$$

$$\left(\frac{k_{g,Ga_2O}}{P_t}\right)P_{Ga_2O} = \frac{1}{2}\left(\frac{k_{g,H_2O}}{P_t}\right)P_{H_2O}$$

$$P_{H_2O} = 2\left(\frac{k_{g,Ga_2O}}{k_{g,H_2O}}\right)P_{Ga_2O}$$

$$\frac{P_{Ga_2O}\left[2\left(\frac{k_{g,Ga_2O}}{k_{g,H_2O}}\right)P_{Ga_2O}\right]^2}{\left(\gamma_{Ga_2O_3}X_{Ga_2O_3}\right)P_{H_2}^2} = e^{\frac{-RT}{\Delta G^o}}$$

$$\left(P_{Ga_2O}\right)^3 = \frac{1}{4}\left(\frac{k_{g,H_2O}}{k_{g,Ga_2O}}\right)^2 P_{H_2}^2 \gamma_{Ga_2O_3} X_{Ga_2O_3} e^{\frac{-RT}{\Delta G^o}}$$

$$X_{Ga_2O_3} \approx \frac{m_{Ga_2O_3}}{m_{PuO_2}} = \frac{N_{Ga_2O_3}M_{Ga_2O_3}}{V\rho_{PuO_2}}$$

$$N_{Ga_2O_3} = \left(\frac{V\rho_{PuO_2}}{M_{Ga_2O_3}}\right)X_{Ga_2O_3}$$

$$-\frac{1}{A}\frac{d\left(N_{Ga_2O_3}\right)}{dt} = -\frac{1}{A}\left(\frac{V\rho_{PuO_2}}{M_{Ga_2O_3}}\right)\frac{d\left(X_{Ga_2O_3}\right)}{dt}$$

$$-\frac{1}{A}\frac{d\left(N_{Ga_2O_3}\right)}{dt}=\left(\frac{k_{g,Ga_2O}}{P_t}\right)P_{Ga_2O}$$

$$-\frac{1}{A}\frac{d\left(N_{Ga_2O_3}\right)}{dt}=\left(\frac{k_{g,Ga_2O}}{P_t}\right)\left[\frac{1}{4}\left(\frac{k_{g,H_2O}}{k_{g,Ga_2O}}\right)^2 P_{H_2}^2\,\gamma_{Ga_2O_3}X_{Ga_2O_3}e^{\frac{-RT}{\Delta G^\circ}}\right]^{\frac{1}{3}}$$

$$-\frac{d\left(X_{Ga_2O_3}\right)}{dt}=\psi X_{Ga_2O_3}^{1/3}$$

where

$$\psi=A\left(\frac{M_{Ga_2O_3}}{V\rho_{PuO_2}}\right)\left(\frac{k_{g,Ga_2O}}{P_t}\right)\left[\frac{1}{4}\left(\frac{k_{g,H_2O}}{k_{g,Ga_2O}}\right)^2 P_{H_2}^2\,\gamma_{Ga_2O_3}e^{\frac{-RT}{\Delta G^\circ}}\right]^{\frac{1}{3}}$$

The final expression is similar to that for a melting sphere described by O'Neil.

$$-\frac{d\left(X_{Ga_2O_3}\right)}{dt}=\psi X_{Ga_2O_3}^{1/3}$$

$$\int_{X_{Ga2O3,0}}^{X_{Ga2O3}}\frac{d\left(X_{Ga_2O_3}\right)}{X_{Ga_2O_3}^{1/3}}=-\psi\int_0^t dt$$

$$\frac{3}{2}\left(X_{Ga_2O_3,0}^{2/3}-X_{Ga_2O_3}^{2/3}\right)=\psi t$$

$$X_{Ga_2O_3}=\left(X_{Ga_2O_3,0}^{2/3}-\frac{2}{3}\psi t\right)^{3/2} \qquad \text{Eq. 3}$$

To assure correctness the relation developed here for Ga_2O partial pressure was compared with that of the original data (Trellue, Figure 2.2.1-2) as shown by Figure 4. The water and Ga_2O mass transfer coefficients were estimated by relationships described in the following.

(3.1.1) Mass transfer from a semi-infinite plate (fixed-bed)

Mass transfer from a semi-infinite plate can represent conditions of minimum mass transfer from a fixed-bed. Boundary layer theory for convective heat transfer from a semi-infinite plate has been described by Kays & Crawford (1980) and can be modified for mass transfer as shown by Equation 4. Equation 4 is applicable for fully developed laminar flow and moderate Schmidt numbers.

$$N_{Sh} = 0.664 N_{Sc}^{1/3} N_{Re}^{1/2} \qquad \text{Eq. 4}$$

$$N_{Sh} = \frac{k_g M_{g,\infty} d_p}{\rho_{g,\infty} D}$$

$$N_{Sc} = \frac{\mu_{g,\infty}}{\rho_{g,\infty} D_{AB}}$$

$$N_{Re} = \frac{d_p v_{g,\infty} \rho_{g,\infty}}{\mu_{g,\infty}}$$

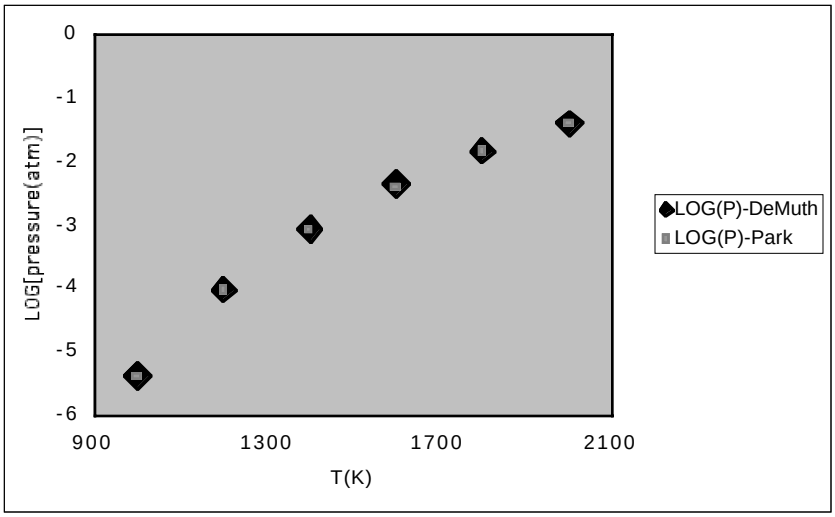

Figure 4. Comparison of Ga_2O partial pressure predicted by this study with original data

Equation 4 can be rearranged to solve for the mass transfer coefficient as shown by Equation 5, and combined with Equation 3 to describe the minimum gallium separation rate by convective mass transfer from a fixed-bed of PuO_2 particles.

$$k_g = \frac{\rho_{g,\infty} D_{AB}}{M_{g,\infty} d_p}\left[0.664\left(\frac{d_p v_{g,\infty} \rho_{g,\infty}}{\mu_{g,\infty}}\right)^{1/3}\left(\frac{\mu_{g,\infty}}{\rho_{g,\infty} D_{AB}}\right)^{1/2}\right] \qquad \text{Eq. 5}$$

(3.1.2) Mass transfer from a particle

Mass transfer from a sphere can be used to represent conditions of maximum mass transport from a mixed-bed. Equation 6 was developed by Ranz & Marshall (1952) to describe evaporation by convection from a drop.

$$N_{Sh} = 2.0 + 0.6 N_{Sc}^{1/3} N_{Re}^{1/2} \qquad \text{Eq. 6}$$

Equation 6 can be solved in terms of the mass transfer coefficient as done with Equation 4, to yield Equation 7.

$$k_g = \frac{\rho_{g,\infty} D_{AB}}{M_{g,\infty} d_p}\left[2 + 0.6\left(\frac{d_p v_{g,\infty} \rho_{g,\infty}}{\mu_{g,\infty}}\right)^{1/3}\left(\frac{\mu_{g,\infty}}{\rho_{g,\infty} D_{AB}}\right)^{1/2}\right] \qquad \text{Eq. 7}$$

(3.1.3) Ga_2O diffusion coefficient

The diffusion of interest is Ga_2O or water into Ar/H_2 where $P_{Ar} >> P_{H2}$ and $P_{Ar} >> (P_{Ga2O}, P_{Ga2O})$. Therefore, as an approximation the diffusion coefficient for Ga_2O diffusing into pure Ar is adequate. The following correlation for the diffusion coefficient was obtained from Equation 11-3.1 of Reid.

$$D_{AB} = 0.001858T^{\frac{3}{2}}\left(\frac{\sqrt{\frac{M_A + M_B}{M_A M_B}}}{P_t \sigma_{AB}^2 \Omega}\right)$$

$$\Omega = \frac{1.06036}{\left(kT/\varepsilon_{AB}\right)^{0.1561}} + \frac{0.19300}{e^{0.47635\left(kT/\varepsilon_{AB}\right)}} + \frac{1.03587}{e^{1.52996\left(kT/\varepsilon_{AB}\right)}} + \frac{1.76474}{e^{3.89411\left(kT/\varepsilon_{AB}\right)}}$$

$$(\varepsilon/k)_{Ga2O} = 1.15(T_b)$$

$$(\varepsilon/k)_{AB} = \sqrt{(\varepsilon/k)_A (\varepsilon/k)_B}$$

Complete thermodynamic data was not available for Ga_2O; consequently, the author developed a rough correlation between boiling temperature and the hard-sphere diameter for similar molecules as shown by Figure 5. Since the mass transfer coefficient was eventually adjusted with actual data this approximate correlation was more than adequate.

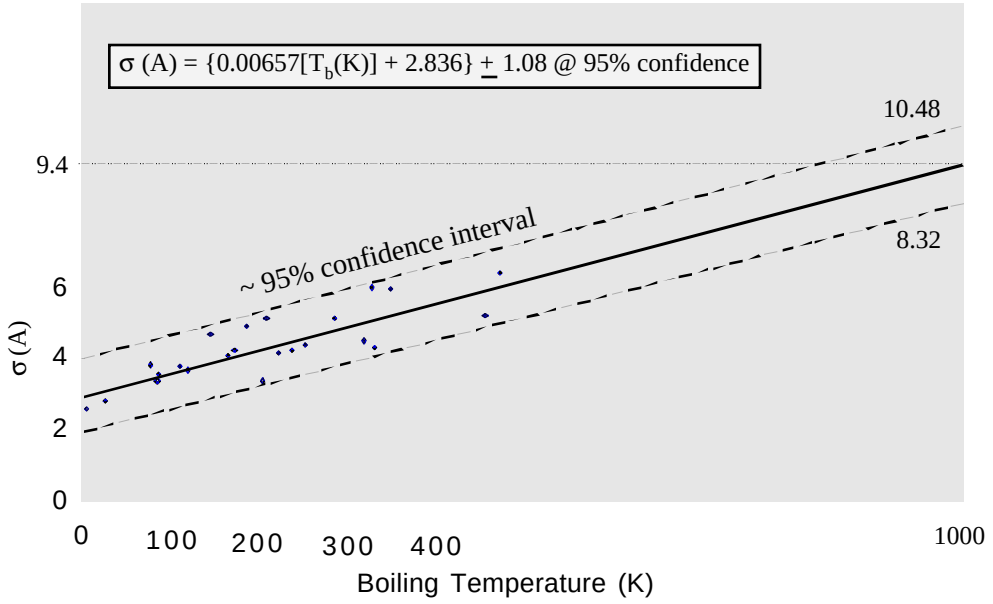

Figure 5. Boiling temperature versus hard sphere diameter for estimation of diffusion coefficient

3.2 Gallium Suboxide Diffusion within Solid PuO_2

Figure 6 shows the concentration profiles for gallium separation controlled by internal particle diffusion. Simplification of the solid-state inter-particle diffusion was accomplished by assuming the gallium exists entirely as the suboxide Ga_2O. This is based on (1) hydrogen diffusion being much faster than gallium, (2) chemical reaction not affecting the gallium loss rate, and (3) the equilibrium conversion of gallium oxide Ga_2O_3 to the suboxide Ga_2O being complete. The equilibrium conversions as estimated are shown in Table 1. Equations 8, 9 and 10 were used to estimate the overall Gibb's free energy of reaction shown by Equation 11.

$$2[Ga]_l + (1/2)[O_2]_g \rightarrow [Ga2O]_g \quad (8)$$

$$[Ga_2O_3]_s \rightarrow 2[Ga]_l + (3/2)[O_2]_g \quad (9)$$

$$2\{2[H_2]_g + [O_2]_g \rightarrow [H_2O]_g\} \quad (10)$$

$$Ga_2O_3]_s + 2[H_2]_g \rightarrow [Ga2O]_g + 2[H_2O]_g \quad (11)$$

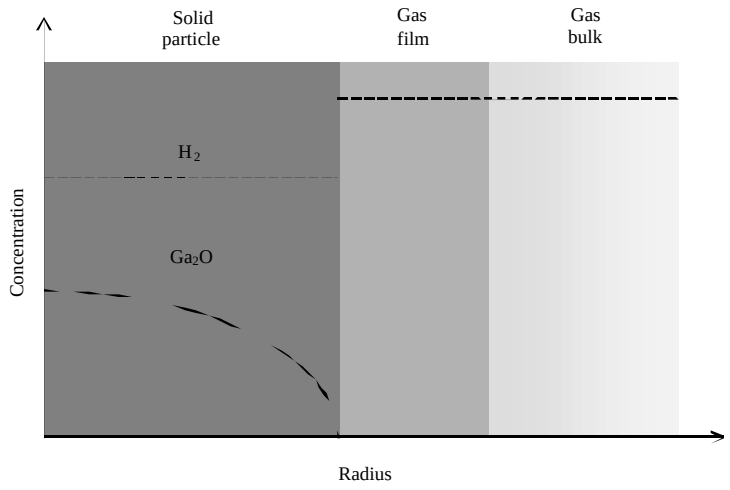

Figure 6. Concentration profiles for internal particle diffusion control

	$\Delta H(298\ K)^a$ J/kgmole	$\Delta G(1000\ K)$ J/kgmole	$\Delta G(1500\ K)$ J/kgmole	$\Delta G(2000\ K)$ J/kgmole
$(Ga_2O)_g$	$3.43x10^8$	$-1.37x10^6$	$-1.17x10^8$	$-2.36x10^8$
$(Ga_2O_3)_s$	$1.08x10^9$	$1.40x10^9$	$1.56x10^9$	$1.70x10^9$
$(H_2O)_g$	$2.86x10^8$	$3.49x10^8$	$3.78x10^8$	$4.07x10^8$
reaction	$-1.65x10^8$	$6.0x10^{36}$	$1.4x10^{32}$	$2.7x10^{29}$
Keq		1.0	1.0	1.0

Table 1. Gibb's free energy of formation

Equation 12 was developed to estimate the extent of Ga_2O_3 to Ga_2O conversion.

$$\Delta G^{T(K)}\left(J/kgmole\right) = \Delta H^{T(298)} - 2.3a_1(T)\log(T) - \frac{a_2}{2}T^2 - \frac{a_3}{6}T^3 - \frac{a_4}{2T} + a_5T - a_6 \quad \text{Eq. X1}$$

$$K_{eq} = e^{-\frac{\Delta G}{RT}}$$

$$e^{-\frac{\Delta G}{RT}} = \frac{\left[\gamma_{Ga_2O}X_{Ga_2O}\right]\left[\gamma_{H_2O}X_{H_2O}\right]^2}{\left[\gamma_{Ga_2O_3}X_{Ga_2O_3}\right]\left[\gamma_{H_2}X_{H_2}\right]^2}$$

$$\gamma_i \approx 1$$

$$+dn_{Ga_2O_3} = +\frac{1}{2}dn_{H_2} = -dn_{Ga_2O} = -\frac{1}{2}dn_{H_2O}$$

$$n_{Ga_2O_3} = (1-\varepsilon)$$
$$n_{H_2} = 2(1-\varepsilon)$$
$$n_{Ga_2O} = \varepsilon$$
$$n_{H_2O} = 2\varepsilon$$

$$X_{Ga_2O_3} = \frac{1-\varepsilon}{3}$$
$$X_{H_2} = \frac{2(1-\varepsilon)}{3}$$
$$X_{Ga_2O} = \frac{\varepsilon}{3}$$
$$X_{H_2O} = \frac{2\varepsilon}{3}$$

$$K_{eq} = \frac{\left[\frac{\varepsilon}{3}\right]\left[\frac{2\varepsilon}{3}\right]^2}{\left[\frac{1-\varepsilon}{3}\right]\left[\frac{2(1-\varepsilon)}{3}\right]^2}$$

$$\varepsilon = \frac{K_{eq}^{1/3}}{1 + K_{eq}^{1/3}} \qquad \text{Eq. 12}$$

where

$$\Delta G_{rxn} = \Delta G_{Ga_2O} - \Delta G_{Ga_2O_3} + 2\Delta G_{H_2O}$$

The constants a_1 through a_6 and enthalpies were obtained from Table 4, Chapter II of Samsonov, where the enthalpies were confirmed with Sheka and Barrow. As shown in Table 1 the extent of conversion to Ga_2O was essentially complete at all temperatures of interest.

Unsteady-state diffusion within a sphere has been solved by Skelland (pp. 21-27) with reasonable convergence for large times as shown by Equation 13, and by Crank (pp. 86-87) with reasonable convergence for short times as shown by Equation 14.

$$\frac{C_{Ga_2O}^{t=0} - \overline{C_{Ga_2O}}}{C_{Ga_2O}^{t=0}} = 1 - \frac{6}{\pi^2}\sum_{n=1}^{\infty}\left[\left(\frac{1}{n^2}\right)e^{\left(-\frac{D\,n^2\pi^2 t}{R^2}\right)}\right] \qquad \text{Eq. 13}$$

$$\frac{C_{Ga_2O}^{t=0} - \overline{C_{Ga_2O}}}{C_{Ga_2O}^{t=0}} = 6\sqrt{\frac{D\,t}{R^2}}\left(\frac{1}{\sqrt{\pi}} + 2\sum_{n=1}^{\infty}\left\{\frac{1}{\sqrt{\pi}}e^{-\left(\frac{nR}{\sqrt{D\,t}}\right)^2} - \left(\frac{nR}{\sqrt{D\,t}}\right)\left[1 - \mathrm{erf}\left(\frac{nR}{\sqrt{D\,t}}\right)\right]\right\}\right) - 3\frac{D\,t}{R^2}$$

Eq. 14

RESULTS

Gallium Suboxide Diffusion within Solid PuO_2

Diffusion in PuO_2 Particle

Actual gallium separation from PuO_2 was reported in Figure 5-6 of Chidester. Based on the data of Chidester, Equation 13 was used to estimate the Ga_2O solid state diffusion coefficient in PuO_2. Table 2 lists the estimated Ga_2O diffusion coefficients. As can be seen from Table 2, the estimated diffusion coefficient is reduced when calculated from later processing times. Based on the earlier elimination of potential competing mechanisms, the decreasing diffusion coefficient can be related to the dominance of gas phase mass transfer at early processing times. While literature based diffusion coefficients for Ga_2O are not available, they are for fission gases in UO_2 which has a crystal structure very similar to PuO_2. These fission product diffusion coefficients range form 10^{-13} to 10^{-15} cm^2/s at ~1473 K as shown in Figure 3-13 of Robertson plus Table 9-4 and Figure 9-3 of Kaufmann. This further supports gas phase mass transfer control at early processing times, and a diffusion coefficient from Table 2 of $9x10^{-13}$ cm^2/s for Ga_2O in PuO_2 at 1473 K.

Processing time (hr)	D (cm^2/s)
0 hr to 4 hrs	$1.0x10^{-10}$
1/2 hr to 4 hrs	$1.9x10^{-11}$
0 hr to 8 hrs	$5.5x10^{-11}$
1/2 hr to 8 hrs	$1.1x10^{-11}$
4 hrs to 8 hrs	$9.1x10^{-13}$

Table 2. Estimated Ga_2O diffusion coefficient in PuO_2 at 1473 K

Gallium Suboxide (Ga_2O) Convective Mass Transfer from the Particle Surface to the Bulk Gas

Fixed bed

In order to judge the adequacy of a fixed bed, some degree of geometry optimization must first be done. Figure 7 shows the results of a sensitivity study that evaluated the effect of fixed bed dimensions upon the Ga_2O mass transfer rate, for a gallium Df of 10,000 (or final concentration of gallium in PuO_2 of ~ 1 ppm). A bed mass of approximately 1-Kg PuO_2 was selected in order to achieve a reasonable processing rate. Overall facility processing must be capable of 3.5 MT-Pu/yr, which at ~300 days/yr operation requires ~13 Kg-PuO_2/day. Criticality limits allow no more than ~4 Kg-PuO_2/furnace, and based on typical furnace dimensions and operations a single bed in a multiple bed furnace should accommodate ~1-Kg PuO_2 in order to minimize handling and maximize Ga_2O mass transfer. Conclusions that can be made from Figure 7 are as follows.

- Based on past experience, it was assumed a 0.6 cm bed depth would be difficult to achieve reliably with minimal plutonium losses. The 0.6 cm was evaluated simply as a point of reference just below the lower end of what is practical.

- The optimum conditions for a bed of 1.2 cm depth, which is likely the minimum bed depth practical, requires a width equal to twice the length.

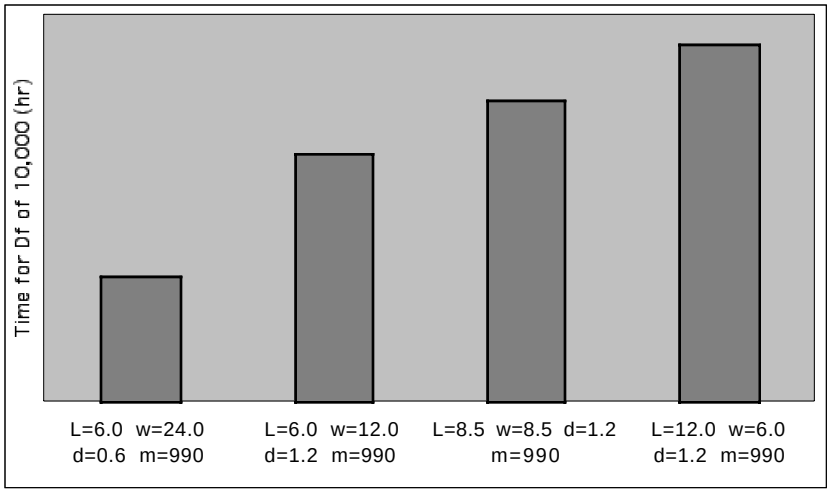

Figure 7. Optimum fixed-bed dimensions

Figure 8 shows the estimated curves for gallium separation based on (1) gas phase convective mass transfer and (2) internal particle diffusion. In addition the actual data from Table 2 is also shown. Since it is assumed gas phase mass transfer controls at early time, the Ga_2O mass transfer coefficient has been adjusted to fit the 1/2-hour data from Table 2. The mass transfer coefficient estimated from the 1/2-hour data was determined to be four times greater than that predicted for a rectangular bed. The actual data was based on a very small PuO_2 sample of 2.5 grams with an irregular surface and bed depth. It is reasonable that modeling the small sample as a solid rectangular bed would underestimate the mass transfer rate. It can be seen that gas phase mass transfer

resistance alone is too rapid and that internal diffusion resistance alone is too slow to account for the galllium separation rate.

Figure 9 shows the estimated curves for gallium separation based on a prototypic size fixed-bed. In this case the mass transfer coefficient was solely based on that estimated for a rectangular bed. Based on gas phase mass transfer control with a maximum hydrogen gas velocity of 6 cm/s at 1473 K, which is critical to prevent PuO_2 entrainment, 12 hours is required to achieve a Df of 10,000. Based on internal particle diffusion control at 1473 K with a prototypic particle diameter of 17.5 microns, approximately 800 hours is required to achieve a Df of 10,000. Based on this information, it will be necessary to increase the processing temperature above 1473 K regardless of the bed type (i.e. fixed or mixed).

Figure 10 shows that increasing the processing temperature from 1473 K to 2000 K reduces the processing time based on internal particle diffusion form ~800 hours to 0.1 hour for a Df of 10,000 and particle diameter of 17.5 microns. Additionally, as shown in Figure 11 at temperature of 2000 K reduces the processing time based on gas phase mass transfer from 12 hours to 0.5 hour for a Df of 10,000.

An additional approach to reducing the processing due to internal particle diffusion is reducing the particle diameter by grinding. As shown in Figure 12, reducing the particle diameter from 17.5 microns to 5 microns at 1473 K reduces the processing time from ~800 hours to 65 hours.

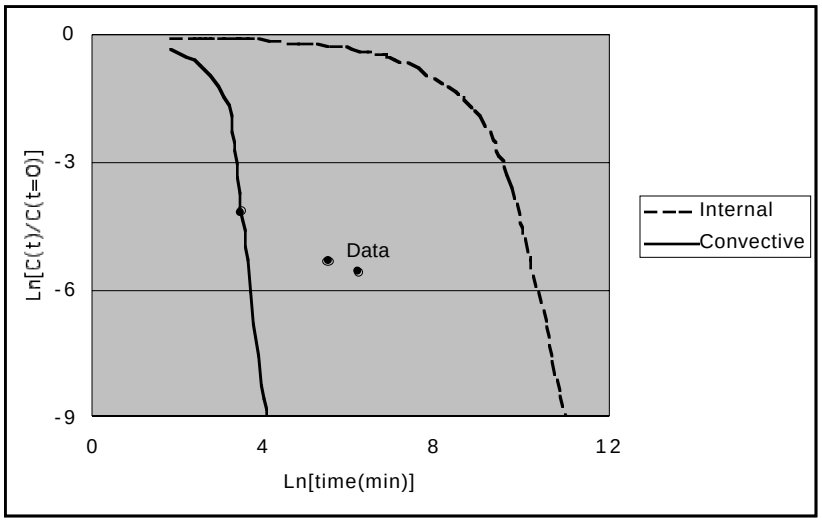

Figure 8. Actual 2.5 gram sample data with predicted gallium separation rates at 1473 K and a particle diameter of 17.5 microns

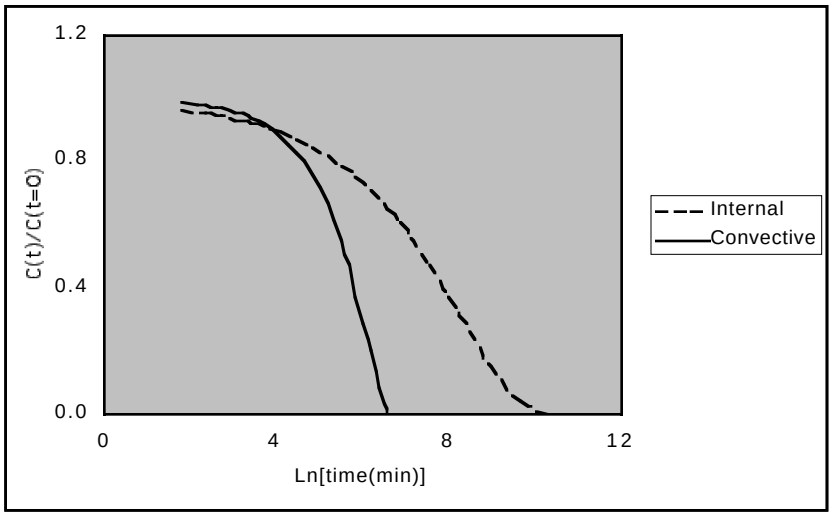

Figure 9. Gallium separation rate for a prototypic fixed-bed (~ 1 kg Pu) at 1473 K and a particle diameter of 17.5 microns

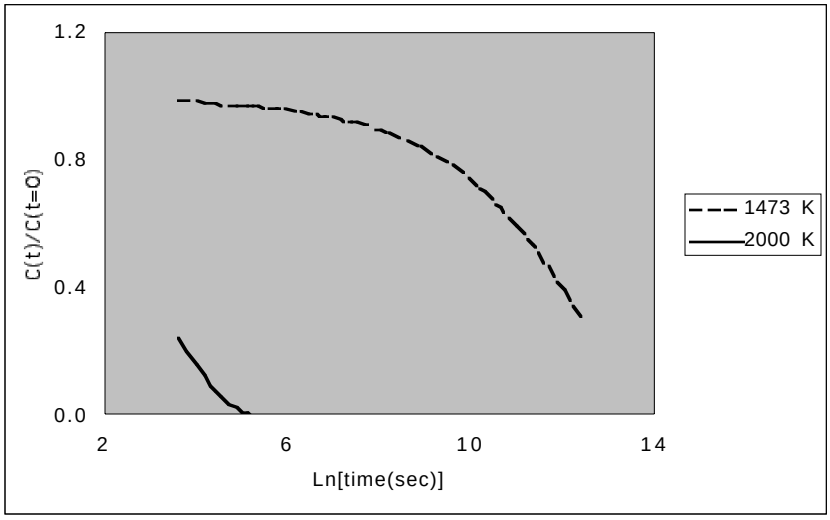

Figure 10. Effect of processing temperature upon internal diffusion for a particle diameter of 17.5 microns

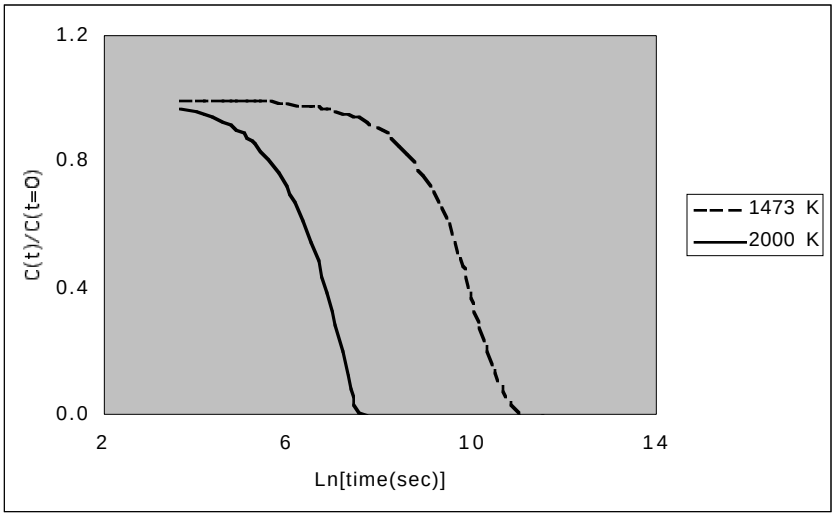

Figure 11. Effect of processing temperature upon gas phase mass transfer for 1473 K and a prototypic fixed-bed (~1 kg Pu)

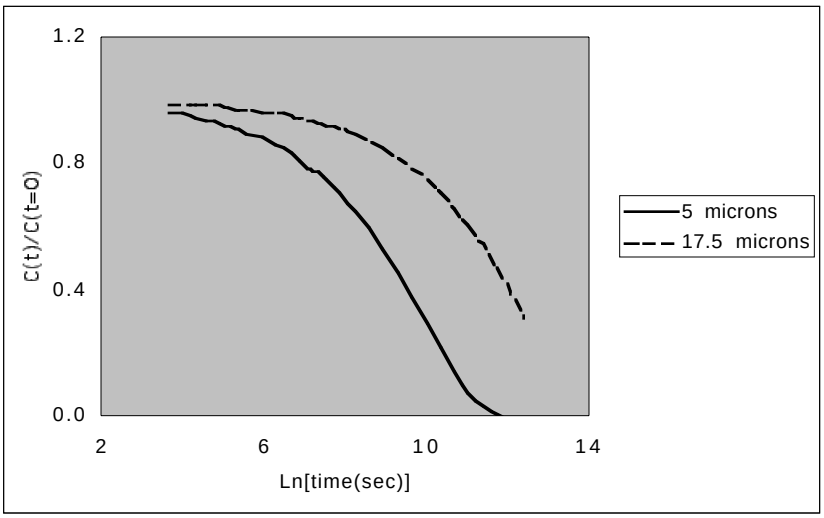

Figure 12. Effect of particle diameter upon internal diffusion at 1473 K

Mixed Bed

In order to determine if a mixed bed has the potential to significantly reduce the processing time, the Ga_2O mass transfer rate from a single particle was estimated so as to represent the minimum rate possible, with the results shown in Table 3. It can be seen from Table 3 that less than one second is required to achieve a Df of 10,000 for a particle. While a mixed-bed would require significantly more time than a single particle, a single particle estimate can still be used to get an idea of the difference between a fixed and mixed bed.

Ga(ppm)	time(seconds)
10,000	0
1000	$9.6x10^{-5}$
100	$1.1x10^{-5}$
10	$1.2x10^{-5}$
1	$1.2x10^{-5}$

Table 3. Gallium separation due to gas phase mass transfer from a 17.5 micron particle at 1473 K

CONCLUSIONS

In conclusion a mixed-bed furnace will provide no significant advatage over a fixed-bed furnace for the removal of gallium from PuO_2 by the TIGR process. The following requirements have led to this conclusion.

- A gallium Df of ~10,000 is sought.
- Processing temperatures above 1500 K will require furnace construction with exotic materials increasing fabrication and operating costs.
- Particle size should not be less than 5 microns, but rather should be maximized to prevent excessive PuO_2 entrainment with associated containment difficulties.
- The hydrogen gas velocity should not exceed 6 cm/s to prevent excessive PuO_2 entrainment with associated containment difficulties.
- The processing temperature and time should be minimized to prevent phase change or excessive PuO_2 sintering with consequent grain growth.
- A processing time of approximately one day per batch based on the simultaneous use of four to five furnaces.

Best on the analysis of this study only an increase in processing temperature above 1473 K can guarantee a reasonable processing time based on internal particle diffusion control. While reducing the particle size to 5 microns can reduce the required temperature increase, particle size reduction alone cannot guarantee a reasonable processing time. Upon increasing the processing

temperature and reducing the particle size to 5 microns, gas phase mass transfer becomes insignificant. Consequently, no clear advantage exists for the use of a mixed-bed furnace over a fixed-bed furnace.

REFERENCES

G.M. Barrow, *General Chemistry*, Wadsworth Publishing, Belmont CA, 1972.

K.M. Chidester, et al., *Nuclear Fuels Technologies Fiscal year 1998 Research and Development Summary of Test Results*, Los Alamos National Laboratory, Los Alamos, NM, LA-UR-98-5355, November 1998.

J. Crank, *The Mathematics of Diffusion*, Clarendon Press, Oxford, 1956.

Kays & Crawford, *Convective Heat and Mass Transfer*, McGraw-Hill, New York, 1980.

A.R. Kaufmann, *Nuclear Reactor Fuel Elements - Metallurgy and Fabrication*, Interscience Publishers of John Wiley & Sons, New York, NY, 1962.

D.G. Kolman, personal communication with author, Los Alamos National Laboratory, Los Alamos, NM, September 1998.

D.G. Kolman, Y. Park, M. Stan, R.J. Hanrahan and D.P. Butt, *An Assessment of the Validity of Cerium Oxide as a Surrogate for Plutonium Oxide Gallium Removal Studies*, Los Alamos National Laboratory, Los Alamos, NM, LA-UR-99-491, February 1999.

P.V. O'Neil, *Advanced Engineering Mathematics*, Wadsworth Publishing, Belmont, CA, 1983.

W.E. Ranz & W.R. Marshall, *Evaporation from Drops, Parts I & II*, Chemical Engineering Progress, Vol. 48, No. 3, pgs 141-146 & 173-180, 1952.

R.C. Reid, J.M. Prausnitz & T.K. Sherwood, *The Properties of Gases and Liquids, 3rd Edition,* McGraw-Hill, 1977.

J. Robertson, *Irradiation Effects in Nuclear Fuels*, Gordon & Breach Science Publishers, New York, 1969.

G.V. Samsonov, *The Oxide Handbook*, IFI/Plenum, New York, 1973.

I.A, Sheka, I.S. Chaus and T.T. Mityureva, *The Chemistry of Gallium*, Elsevier Publishing, New York, 1966.

A.H.P. Skelland, *Diffusional Mass Transfer*, John Wiley & Sons, New York, 1974.

H.R. Trellue, et al., *Nuclear Fuels Technologies Fiscal Year 1997 Research and Development Test Results*, Los Alamos National Laboratory, Los Alamos, NM, LA-UR-97-4423, November 1997.

The White House, Office of the Press Secretary, 26 January 1996, http://www.pub.whitehouse.gov/uri-res/I2R?urn:pdi://oma.eop.gov.us/1996/2/2/3.text.1

The White House, Office of the Press Secretary, 1 September 1998, http://www.pub.whitehouse.gov/urires/I2R?urn:pdi://oma.eop.gov.us/1998/9/2/15.text.1